A joint theoretical and kinetic investigation on the fragmentation of (N-halo)-2-amino cycloalkanecarboxylates

ARTICLE *in* CHEMICAL PHYSICS · JUNE 2002

Impact Factor: 1.65 · DOI: 10.1016/S0301-0104(02)00487-1

6 AUTHORS, INCLUDING:

Moisés Canle López
University of A Coruña
124 PUBLICATIONS **1,397** CITATIONS
SEE PROFILE

J. Arturo Santaballa
University of A Coruña
98 PUBLICATIONS **1,235** CITATIONS
SEE PROFILE

J. R. Sambrano
São Paulo State University
91 PUBLICATIONS **1,422** CITATIONS
SEE PROFILE

ELSEVIER

Chemical Physics 280 (2002) 1–14

Chemical Physics

www.elsevier.com/locate/chemphys

A joint theoretical and kinetic investigation on the fragmentation of (*N*-halo)-2-amino cycloalkanecarboxylates

Joaquim J. Queralt [a,*], Juan Andrés [a,1], Moisés Canle L. [b,2], J. Hermógenes Cobas [b], Juan A. Santaballa [b], Julio R. Sambrano [c,3]

[a] *Departament de Ciències Experimentals, Universitat Jaume I, Campus de Riu Sec, E-12071 Castelló, Spain*

[b] *Departamento de Química Física e Enxeñería Química I, Universidade da Coruña, Rúa Alejandro de la Sota, 1, E-15008 A Coruña, Spain*

[c] *Departamento de Matemática, Universidade Estadual Paulista – UNESP, Caixa Postal 473, CEP 17033 360 Bauru, São Paulo, Brazil*

Received 23 January 2002; in final form 2 April 2002

Abstract

A combined theoretical and experimental study to elucidate the molecular mechanism for the Grob fragmentation of different (*N*-halo)-2-amino cyclocarboxylates with the nitrogen atom in exocyclic position: (*N*-Cl)-2-amino cyclopropanecarboxylate (**1**), (*N*-Cl)-2-amino cyclobutanecarboxylate (**2**), (*N*-Cl)-2-amino cyclopentanecarboxylate (**3**) and (*N*-Cl)-2-amino cyclohexanecarboxylate (**4**), and the corresponding acyclic compounds, (*N*-Cl)-2-amino isobutyric acid (**A**), (*N*-Cl)-2-amino butyric acid (**B**), has been carried out.

The kinetics of decomposition for these compounds and related bromine derivatives were experimentally determined by conventional and stopped-flow UV spectrophotometry. The reaction products have been analyzed by GC and spectrophotometry. Theoretical analysis is based in the localization of stationary points (reactants and transition structures) on the potential energy surface. Calculations were carried out at B3LYP/6-31+G* and MP2/6-31+G* computing methods in the gas phase, while solvent effects have been included by means the self-consistent reaction field theory, PCM continuum model, at MP2/6-31+G* and MP4/6-31+G*//MP2/6-31+G* calculation levels.

Based on both experimental and theoretical results, the different Grob fragmentation processes show a global synchronicity index close to 0.9, corresponding to a nearly concerted process. At the TSs, the N–Cl bond breaking is more advanced than the C–C cleavage process. An antiperiplanar configuration of these bonds is reached at the TSs, and this geometrical arrangement is the key factor governing the decomposition. In the case of **1** and **2** the ring strain prevents this spatial disposition, leading to a larger value of the activation barrier.

Natural population analysis shows that the polarization of the N–Cl and C–C bonds along the bond-breaking process can be considered the driving force for the decomposition and that a negative charge flows from the carboxylate

* Corresponding author. Tel.: +34-964-728083; fax: +34-964-728066.

E-mail addresses: queralt@exp.uji.es (J.J. Queralt), andres@exp.uji.es (J. Andrés), mcanle@udc.es (Moisés Canle L.), hermocob@mail2.udc.es (J. Hermógenes Cobas), arturo@udc.es (J.A. Santaballa), sambrano@fc.unesp.br (J.R. Sambrano).

[1] Tel.: +34-964-728083; fax: +34-964-728066.

[2] Tel.: +34-981-167000; fax: +34-981-167065.

[3] Tel.: +55-14-2216086; fax: +55-14-2219386.

0301-0104/02/$ - see front matter
PII: S0301-0104(02)00487-1

group to the chlorine atom to assist the reaction pathway. A comparison of theoretical and experimental results shows the relevance of calculation level and the inclusion of solvent effects for determining accurate unimolecular rate coefficients for the decomposition process. © 2002 Published by Elsevier Science B.V.

1. Introduction

Decomposition processes, as proposed by Grob and Baumann [1], imply the breaking of a molecule a–b–c–d–X into three fragments a–b, c=d and X, the first being the "electrofuge" and the last the "nucleofuge" [2]. Experimental kinetic studies on a particular case of this rearrangement, fragmentation of acyclic (*N*-Cl)-2-amino acids in solution, have been carried out [3–15]. The observed rates coefficients for the fragmentation of (*N*-X)-2-amino cycloalkane carboxylates (X = Cl and Br) show anomalous values, exceeding those of their unstrained analogs, which may arise from the fact that the cyclic substrates bear a strain energy. Usually, such high rate coefficients have been interpreted in terms of a lowering of the energy barrier to reaction due to partial strain relief at the transition structure [16]. This interpretation has recently been questioned by additional studies showing that these effects seem to stem from bond length and bond angle deformation, leading to orbital rehybridization that results in frontier orbitals becoming more amenable for bonding [17,18]. However, since the need for antiperiplanarity in the transition structure (TS) has been claimed for this kind of process to take place [19] the question arises in how the geometrical deformation affects the reaction mechanism.

Experimental work and complementary theoretical studies show the reaction is unimolecular and obeys a first-order rate law (see Scheme 1) [20–25]. Following these studies a fundamental interest appears to understand in detail the mechanism of Grob fragmentation of (*N*-X)-2-amino cycloalkane carboxylates. A deep understanding at a molecular level of the chemical events can be obtained from kinetic studies and complementary quantum mechanical characterization of potential energy surface (PES). The geometries and energies of stationary points on the PES can be calculated

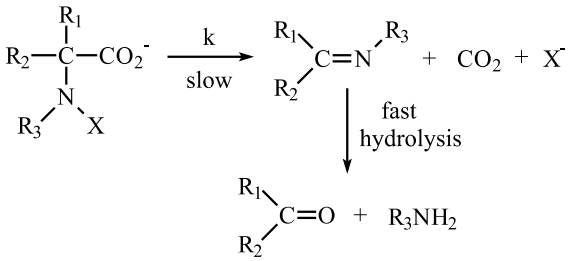

Scheme 1.

and the rate coefficients of a given reaction pathway can be obtained.

In view of these facts and in the framework of a wider project aiming to clarify the mechanisms determining the fate of halogenated derivatives of biologically relevant compounds, we have carried out the first combined experimental and theoretical investigation on the reaction mechanism for the Grob fragmentation of cyclic **1**–**4** and acyclic (*N*-halo)-2-amino alkanecarboxylates **A** and **B** (see Fig. 1). The present paper is organized as follows: in Sections 2 and 3 the experimental details and computational methods are given, respectively, in Section 4 both experimental and theoretical results are presented and discussed. Finally, a short section of conclusions closes the paper.

2. Experimental

(*N*-X)-2-amino acids are ambidentate ligands toward H^+, showing two macroscopic acid–base equilibria, which implies four microscopic acid–base equilibria and one tautomerization equilibrium [26]. Considering the thermodynamics of ionization of (*N*-X)-2-amino acids [3,10], the conclusion is drawn that within the pH range used in this study, these are present in the form of carboxylate anions. Six compounds, depicted in Fig. 1, have been selected: 2-(*N*-Cl)-amino cyclopropanecarboxylate (**1**), 2-(*N*-Cl)-amino cyclobutanecarboxylate (**2**), 2-(*N*-Cl)-amino cy-

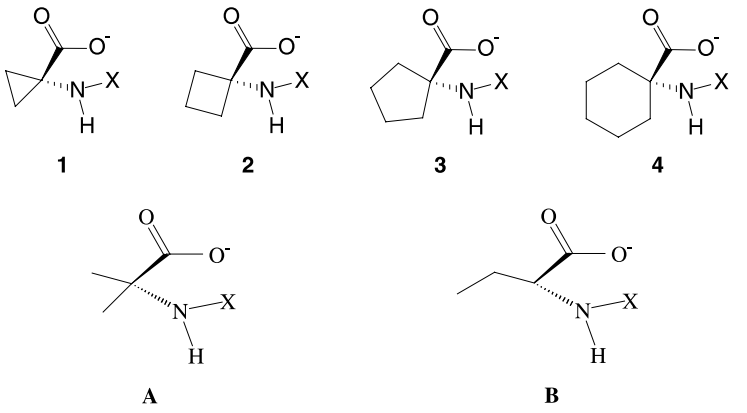

Fig. 1. (*N*-Cl)-2-amino cyclopropanecarboxylate (**1**), (*N*-Cl)-2-amino cyclobutanecarboxylate (**2**), (*N*-Cl)-2-amino cyclopentanecarboxylate (**3**) and (*N*-Cl)-2-amino cyclohexanecarboxylate (**4**) with the nitrogen in exocyclic position, (*N*-Cl)-2-amino isobutyric acid (**A**) and (*N*-Cl)-2-amino butyric acid (**B**).

clopentanecarboxylate (**3**) and 2-(*N*-Cl)-amino cyclohexanecarboxylate (**4**) with the nitrogen in exocyclic position; in order to compare the behavior of **1**–**4** with that of acyclic structures, two open chains have been considered: (*N*-Cl)-2-amino isobutyric acid (**A**) and (*N*-Cl)-2-amino butyric acid (**B**). These acyclic systems can be obtained from a breaking process of the three-membered ring **1**. In addition, rate coefficients for related bromine derivatives of **3**, **4**, **A** and **B** compounds have been also experimentally obtained.

(*N*-X)-2-amino cycloalkanecarboxylic acids were generated in situ by reacting aqueous chlorine solutions with the corresponding α-amino acids, a reaction known to proceed to completion within milliseconds at room temperature and near neutral pH values [6,11]. Aqueous chlorine solutions were prepared by adjusting appropriate NaOCl solutions to the desired pH. The way in which the concentration of aqueous chlorine was titrated, and the detailed experimental procedure, have been described elsewhere [3]. All other chemicals were of the highest purity commercially available, and used without further purification. The pH of the medium was adjusted with 10 mM CH_3COO^-/CH_3COOH, $H_2PO_4^-/HPO_4^{2-}$, $B(OH)_3/B(OH)_4^-$ and HCO_3^-/CO_3^{2-} buffer solutions. The ionic strength was kept to 500 mM using $NaClO_4$ as inert electrolyte.

Unless otherwise stated, the reactions were monitored at 298.0 K by measuring the decrease in the absorption of the corresponding (*N*-X)-2-amino acid (ca. 255 nm) in a conventional Beckman UV–Vis spectrophotometer or in a single-mixing Hi-Tech Scientific SF-61 stopped-flow spectrophotometer. The reagents and the cell holder were water-flow thermostated to within 0.1 K. pH values were measured with an adequately calibrated combined glass electrode, with an accuracy of 0.01 units.

The integrated first-order rate equation was fitted to experimental data using a standard statistical package allowing non-linear least-squares treatment. The values reported for the first-order rate coefficients are an average of those obtained for three kinetic runs, their accuracy is better than 5%. In general, the main products of the unimolecular fragmentation of (*N*-X)-2-amino carboxylates are CO_2, Cl^-, and NH_3 and a carbonyl compound, these last two arising from hydrolysis of the corresponding imines (see Scheme 1). The (*N*-X)-α-amino carboxylates used for product analysis were generated following the same method as for the kinetic runs, using a phosphate buffer to get pH ca. 7, and the fragmentation reaction was left to proceed completely.

Ammonia analysis was carried out using a NH_3 selective electrode, properly calibrated with NH_4Cl. For this purpose, the solutions were taken to 200 mM NaOH, in order to keep within the range of ionic strength admissible for the NH_3 electrode. The analysis of the cyclic ketones derived from (*N*-X)-2-amino cycloalkanecarboxylates was per-

formed by gas chromatography, using a Konik Instruments-3000 GC apparatus, equipped with a FID detector. A 0.32 mm i.d. × 30 m DB-WAX capillary column, with a 0.5 μm film thickness (J & W Scientific) operated isothermally at 373 K in the case of (*N*-X)-2-amino cyclohexanecarboxylate and at 358 K in the case of (*N*-X)-2-amino cyclopentanecarboxylates. The carrier gas was helium (4.2 ml min^{-1}). The retention times (t_R) of the reaction products, compiled in Table 1, and the linearly of response of the detector to all of them were checked by comparison with authentical samples, and appropriate linear calibrations used to calculate the reaction yields. 2-Hexanone ($t_R = 2.1$ min) was injected as internal standard in all samples.

Alternatively, the yields of cyclic ketones were alternatively obtained by generation of the corresponding (2,4)-dinitrophenylhydrazones, that were then extracted with hexane and their absorbance measured at 340 nm [27]. The absorbance was checked against an appropriate calibration line obtained following the same procedure with a commercial sample of the corresponding ketone. The nature of the cyclic ketones formed was confirmed by forming the corresponding dimethones and measuring their melting points, which were in good agreement with those reported in the literature [28]. Under the described conditions, the product yields obtained upon Grob fragmentation of **3** and **4** at different pH values are compiled in Table 1. Subsequent reactions of the primary products have not been studied.

Considering the high yield of ammonia obtained in all cases and the low yields of carbonyl compounds found when using 1:1 Cl:N ratio for **3**, **4** and **B**, it seems that although the fragmentation proceeds to completion, the ketones tend to undergo a secondary process, which does not take place in the case of aldehydes. Since for **3** and **4** the yield of carbonyl product grows as the Cl:N ratio increases, such secondary process would not be a further oxidation of the ketone, but rather take place in the presence of excess amino acid, for which there is precedence [29]. The possible presence of (*N*,*N*)-di-Cl-2-amino carboxylates in the experiments with 10:1 and 1:1 Cl:N ratios would not interfere in the case of **3** and **4**, since it has been shown that the presence of a –H substituent on the C_2 is necessary for (*N*,*N*)-di-Cl-2-amino carboxylates to yield nitriles with one carbon atom less than the starting (*N*,*N*)-di-Cl-2-amino carboxylate [30–37]. In turn, if a (*N*,*N*)-di-Cl-2-amino carboxylate derived from **3** or **4** is formed these would lead to the corresponding ketone, upon hydrolysis of the corresponding (*N*-Cl)-imine, which explains the growth in the yield or carbonyl compound as the Cl:N ratio increases.

3. Computational and theoretical methods

Calculations were carried out with the GAUSSIAN98 package program [38]. DFT methodology with the B3LYP [39,40] hybrid

Table 1
Yields of final products obtained for the Grob fragmentation of **3**, **4**, **A** and **B** at pH *ca.* 7

(*N*-Cl)-2-amino carboxylate	% NH_3, Cl:N ratio	% Carbonyl product	
		Product	% Yield, method, Cl:N ratio
3	–	Cyclopentanone	100%, GC, 10:1 41%, GC, 1:1 12%, GC, 1:10
4	92%, 1:1	Cyclohexanone	100%, GC, 10:1 41%, GC, 1:1 12%, GC, 1:10
A	79%	Propanaldehyde	80%, spectrophotometric, 1:1
B	82%	Acetone	41%, spectrophotometric, 1:1

For 3 and 4 the GC retention times (t_R) obtained were 4.1 min.

functional and MP2 and MP4 perturbation theory [41] and 6-31+G* basis set have been selected. In the present study, a previous conformational analysis with geometrical optimizations of the stationary points along the PES was carried out using the B3LYP method. A full geometry optimization and frequency calculations in the gas phase have been carried out at the B3LYP and MP2 levels.

The vast majority of chemical reactions are carried out in solution, and the study of solvent effects can yield valuable information about their reaction mechanisms. To study the solvent effect we used the self-consistent reaction field (SCRF) method. In this methodology the solute is placed in a cavity surrounded by a continuum with a dielectric constant equal to 78.4. The approach used to compute the solvation energy is based on the polarized continuum model (PCM), as implemented in GAUSSIAN98, and developed by Tomasi et al. [42,43]. These effects were taken into account with full MP2/6-31+G* and single point energy MP4/6-31+G*//MP2/6-31+G* calculations.

Each stationary point on the PES is characterized by an index which is equal to the number of negative eigenvalues of the Hessian matrix (0 for a minimum, 1 for a saddle point). The TSs were found using an "eigenvalue following" optimization method [44,45]. The nature of each stationary point was established by calculating and diagonalizing the Hessian matrix (force constant matrix). The TSs were characterized by means of a normal mode analysis at MP2/6-31+G* level of calculation. The unique imaginary frequency associated with the transition vector (TV) [46] has been characterized. This analysis also provides thermodynamic quantities such as zero point vibrational energy (ZPVE), temperature corrections ($E(T)$) and the absolute entropy ($S(T)$) [47], and consequently the rate coefficient can be estimated. Temperature corrections and absolute entropies were obtained assuming ideal gas behavior, from the harmonic frequencies and moments of inertia by standard methods [48].

The transition state theory (TST) [49,50], used almost universally by chemists interested in reaction mechanisms [51,52] was employed to calculate the kinetic parameters derived from the theoretical study. The rate coefficient ($k(T)$) was computed by means of the standard equation [49,53–59]:

$$k(T) = \chi \frac{k_B T}{h} e^{-\Delta G^{\neq}/RT}, \tag{1}$$

where χ is the transmission coefficient, assumed to be unity, $\Delta G^{\neq}$ is the Gibbs free energy change between the reactant and its corresponding transition structure, and k_B and h are the Boltzmann and Planck constants, respectively. $\Delta G^{\neq}$ was calculated as $\Delta G^{\neq} = \Delta H^{\neq} - T \cdot \Delta S^{\neq}$, taking into account that

$$\Delta H^{\neq} = \mathrm{PEB} + \Delta\mathrm{ZPVE} + \Delta E(T), \tag{2}$$

where PEB is the potential energy barrier and ΔZPVE and $\Delta E(T)$ are the differences of ΔZPVE and temperature corrections between the TS and the corresponding reactant, respectively.

The bond order (B) has been used to obtain a deeper insight into the extent of bond formation/bond breaking along a reaction pathway [60–62]. To follow the nature of the decomposition process, the Wiberg bond indexes [63] have been computed by using the natural bond orbital (NBO) [64,65] analysis as implemented in GAUSSIAN98. Several bond breaking and bond forming processes are involved in the fragmentation, and the global nature of the fragmentation process can be monitored using the synchronicity (Sy) concept proposed by Moyano et al. [66]; Sy values close to 1 indicate a synchronous process. Sy is defined as

$$\mathrm{Sy} = 1 - \left\{ \sum_{i=1}^{n} \frac{|\delta B_i - \delta B_{\mathrm{av}}|}{\delta B_{\mathrm{av}}} \Big/ (2n-2) \right\}, \tag{3}$$

where n is the number of bonds directly involved in the reaction. The relative variation of the bond index is obtained from

$$\delta B_i = \frac{B_i^{\mathrm{TS}} - B_i^{\mathrm{R}}}{B_i^{\mathrm{P}} - B_i^{\mathrm{R}}}, \tag{4}$$

where the superscripts TS, R and P refer to the TS, reactant and product, respectively. The average value is therefore

$$\delta B_{\mathrm{av}} = n^{-1} \sum_{i=1}^{n} \delta B_i. \tag{5}$$

The percentage of evolution of the bond order along the chemical step has been calculated as

$$\%\mathrm{Ev} = \delta B_i \times 100. \quad (6)$$

4. Results and discussion

4.1. Experimental study

The rate coefficient is independent of the acidity of the medium in a broad range of pH, as expected for this kind of mechanism [8]. Such interval was found to be shorter for (*N*-Br)- than for (*N*-Cl)-compounds due to the enhanced reactivity of the former. The observed rate coefficients are independent of the concentration of both α-amino acid and hypohalous acid, from which the compounds under study were generated. Similarly, ionic strength was shown not to have any influence on the fragmentation process. The reaction rate law is simply given by

$$r = k_{\mathrm{obs}}[(N\text{-X})\text{-2-amino alkane carboxylate}]. \quad (7)$$

The values of the rate coefficients (k_{obs}) for the Grob fragmentation of **1**, **3**, **4**, **A** and **B** and related bromine compounds are shown in Table 2 and correspond to a relatively fast process.

Different mechanistic alternatives for the Grob fragmentation process have been previously discussed and discarded for (*N*-X)-2-amino acids with open-chain substituents [8]. All the arguments used in such discussion are of application in the present case of (*N*-X)-2-amino acids with cyclic substituents. On this basis, the conclusion can be drawn that the C_1–C_2 and N–X bond breaking processes and the C_2=N bond forming process take place in a slightly asynchonous manner.

In all cases, a general-base catalyzed process, corresponding to an $A_{xh}D_HD_N$ process has been observed in alkaline medium, at pH values higher than the upper limits indicated in Table 2. Under the conditions used in our study, this elimination process can be neglected [4,9,14].

The accepted kinetic mechanism, which agrees with the experimental data, is shown in Scheme 1 [8]. It follows that the observed rate coefficient (k_{obs}) coincides with the rate coefficient (k) of the elementary Grob fragmentation step of the reaction mechanism [67].

In order to assess the effect of the presence of cyclic substituents, **A** must be taken as a reference. Thus, for (*N*-X)-2-amino cycloalkanecarboxylates $k(\mathbf{3}) < k(\mathbf{A})$ and $k(\mathbf{4}) \gg k(\mathbf{A})$, and for (*N*-Cl)-2-amino cycloalkanecarboxylates also holds $k(\mathbf{1}) > k(\mathbf{A})$. The long-range electronic effect of alkyl substituents is very small or negligible, so the observed tendencies must be attributed to distortions induced in the TS by the presence of cyclic substituents, presumably angular changes due to strain, affecting the achievement of the antiperiplanar configuration needed for reaction.

Table 2
Rate coefficients at 298 K for the Grob fragmentation of different (*N*-X)-2-amino carboxylates, nucleofuge effect (N.E. = $k_{\mathrm{N\text{–}Br}}/k_{\mathrm{N\text{–}Cl}}$), and activation parameters for (*N*-Cl)-2-amino carboxylates

Compound	$k_{\mathrm{N\text{–}Cl}} \times 10^2$ (s^{-1})	$k_{\mathrm{N\text{–}Br}} \times 10^2$ (s^{-1})	N.E.
1	7.2 ± 0.7 $6.54 < \mathrm{pH} < 8.60$	–	–
3	1.12 ± 0.03 $5.99 < \mathrm{pH} < 10.06$	9.8 ± 0.6 $6.76 < \mathrm{pH} < 9.37$	9
4	10.0 ± 0.1 $5.65 < \mathrm{pH} < 9.78$	70 ± 2 $6.80 < \mathrm{pH} < 9.28$	7
A	1.5 ± 0.2 $2.96 < \mathrm{pH} < 14.00$	12.2 ± 0.4 $8.09 < \mathrm{pH} < 9.56$	8
B	0.038 ± 0.001 $5.50 < \mathrm{pH} < 9.10$	0.14 ± 0.2 $8.50 < \mathrm{pH} < 9.90$	4

Assuming the strain energies of cyclic substituents have similar values or follow a tendency similar to that of covalently bonded cyclic molecules [68,69], the fragmentation of **1** should be highly disfavored relative to those of **3** or **4**. This is contrary to the experimental observation. In addition, cyclopropanone was not observed as final product for **1**. On this basis, it can be concluded that the decomposition of **1** takes place through a mechanism other than the fragmentation. A possible alternative would be a mechanism leading to ethylene [70–73].

An analysis of the nucleofuge effect (N.E.), defined as $\text{N.E.} = k_{\text{N–Br}}/k_{\text{N–Cl}}$, presented in Table 2 shows that bromide is better nucleofuge than chloride, and slightly accelerates the fragmentation. This effect is higher for **3**, **4** and **A** than **B**, respectively. This indicates that the degree of N–X bond breaking is twice as much in the case of (*N*-X)-2-amino carboxylates fully substituted at C_2. No difference is observed in this case between **3**, **4**, and **A**, therefore, the presence of a cyclic substituent does not significantly affect the degree of N–X bond breaking process.

The introduction of alkyl substituents on the C_2 leads to moderate increase in the fragmentation rate, as shown by the ratios $k_{\text{N–Br}}(\mathbf{A})/k_{\text{N–Br}}(\mathbf{B}) \approx 90$ and $k_{\text{N–Cl}}(\mathbf{A})/k_{\text{N–Cl}}(\mathbf{B}) \approx 40$ (see Table 2). Since the methyl group is a poor charge donor, C_2 is an

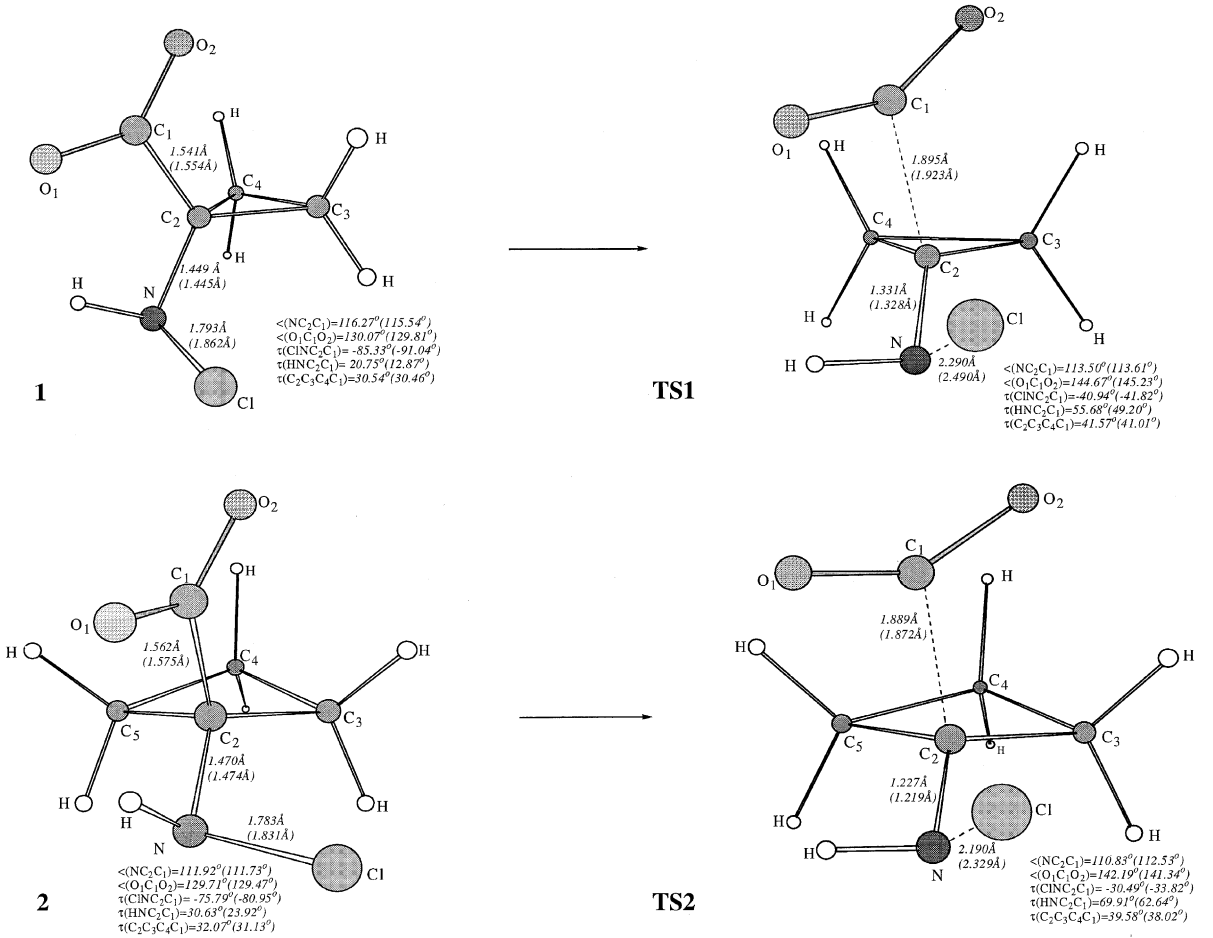

Fig. 2. Optimized geometries of the stationary points (reactants and transition structures) for **1** and **2**. Results obtained with MP2/6-31+G*computing method (in parentheses, results obtained with B3LYP/6-31+G*).

electrophilic center, accepting charge, and as a reaction center it is quite sensitive to changes in electronic density. As the observed effect is higher for (*N*-Br)- than for (*N*-Cl)-2-amino carboxylates, it follows that the donating effect is more relevant in the case of (*N*-Br)-2-amino carboxylates, which points to a higher demand of electronic density at the C_2 in the TS.

4.2. Theoretical results

4.2.1. Geometries and transition vectors

Relevant geometrical parameters of the stationary points and the corresponding structures are depicted in Figs. 2–4.

An analysis of the reactants renders small differences between the values obtained at the MP2 and DFT methods. Nevertheless, the values of C_1–C_2 and N–Cl bond lengths, as well as the $\tau(ClNC_2C_1)$ and $\tau(HNC_2C_1)$ dihedral angles, are computing method dependent. For example, the larger difference found for C_1–C_2 bond distance was 0.045 Å for compound **4**, and for the N–Cl bond length was 0.09 Å for systems **3** and **4**. Differences up to 6° in the values of $\tau(ClNC_2C_1)$ dihedral angle and of up to 8° in the $\tau(HNC_2C_1)$ dihedral angle are found for **1** compound.

The geometrical parameters of TSs are even more dependent on computing methods. Thus, the difference observed for the values of N–Cl dis-

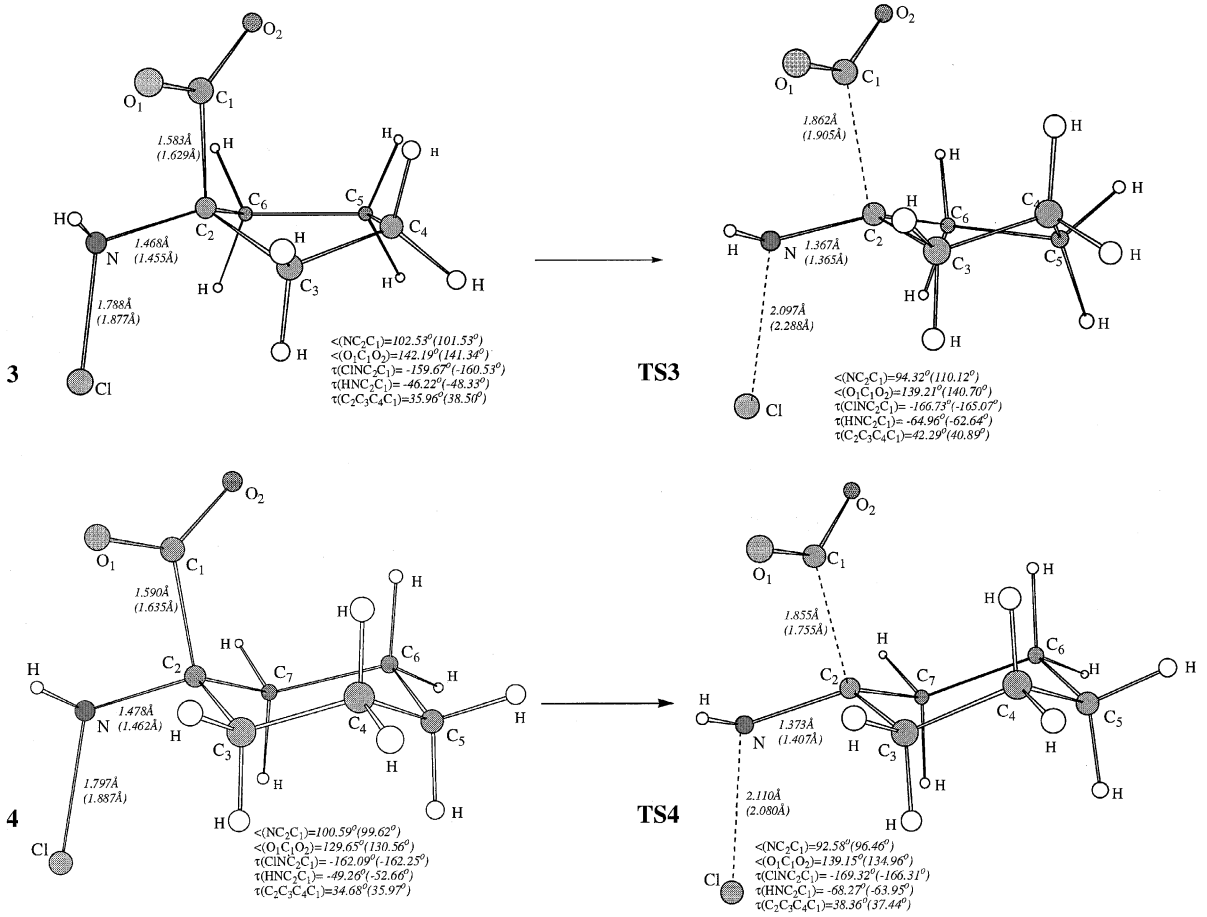

Fig. 3. Optimized geometries of the stationary points (reactants and transition structures) for **3** and **4**. Results obtained with the MP2/6-31+G* computing method (in parentheses, results obtained with the B3LYP/6-31+G* method).

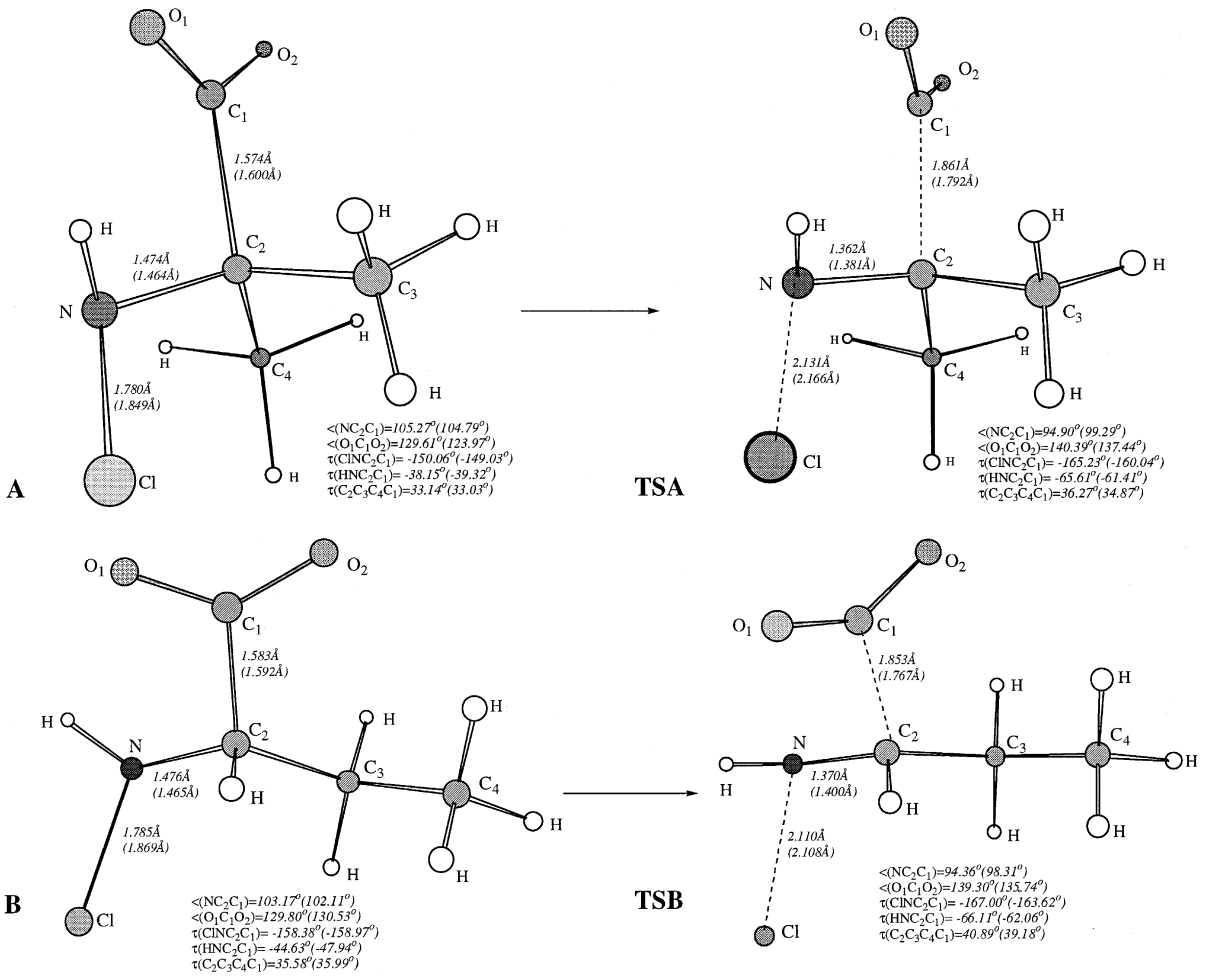

Fig. 4. Optimized geometries of the stationary points, (reactants and transition structures) for **A** and **B**. Results obtained with the MP2/6-31+G* computing method (in parentheses, results obtained with the B3LYP/6-31+G* method).

tances is near to 0.2 Å for **TS1** and **TS3**. At B3LYP level, the value of the $\langle(NC_2C_1)$ bond angle increases up to 16° for the **TS3,** and the values of $\tau(ClNC_2C_1)$ dihedral angle until 5° for **TSA**.

Among the most important geometrical parameters, the $\tau(ClNC_2C_1)$ dihedral angle is a measure of the antiperiplanarity between the NCl and C_1C_2 bonds. The values range from 150.06° to 169.32° and from 149.03° to 166.31°, respectively, at the MP2 and B3LYP levels of calculations, for **3**, **4**, **A** and **B**. Thus, a near antiperiplanar conformation is reached at the TS of these compounds. However, the strain of the three-, **1**, and four-membered rings, **2**, prevents the corresponding TSs to reach the $\tau(ClNC_2C_1)$ dihedral angle value close to 180°.

Table 3 compiles the values of the imaginary frequencies and the components of the corresponding transition vectors of the different TSs. The imaginary frequency values are in the range 477–574 and 179–425 cm^{-1} for the MP2 and B3LYP levels of calculation, respectively. The main components of the transition vector are the C_1–C_2 and N–Cl distances, with a small contribution of the $\tau(ClNC_2C_1)$ dihedral angle.

Table 3
Imaginary frequencies (cm^{-1}) and component of the transition vector (C)H for TS1, TS2, TS3, TS4, TSA and TSB

	TS1	TS2	TS3	TS4	TSA	TSB
Imaginary frequency	−574.19i (−425.55i)	−642.33i (−374.90i)	−478.46i (−192.31i)	−477.151 (−179.639i)	−486.99i (−210.30i)	−490.97i (−198.53i)
C						
$r(C_1C_2)$	0.581 (0.674)	0.553 (0.607)	0.587 (0.554)	0.618 (0.483)	0.558 (0.557)	0.562 (0.523)
r(NCl)	0.585 (0.484)	0.565 (0.565)	0.675 (0.685)	0.601 (0.684)	0.663 (0.598)	0.657 (0.685)
$\tau(ClNC_2C_1)$	0.033 (−0.059)	0.164 (0.282)	0.008 (−0.199)	−0.004 (−0.136)	−0.151 (−0.192)	0.245 (0.226)

Results obtained with MP2/6-31+G* computing method (in parentheses, results obtained with B3LYP/6-31+G*).

4.2.2. Bond order analysis

The values of the Wiberg bond indexes and the percentages of evolution for the bond order and synchronicities along the bond breaking/bond making processes are reported in Table 4. At the TSs, the highest percentages of evolution of the bond order correspond to N–Cl and C_1–C_2 bonds, which are being broken. The values of evolution for C_2=N, C_1–O_1 and C_1–O_2 bonds are always lower than for N–Cl and C_1–C_2 bonds. Results of percentage of evolution obtained with the two levels of calculation employed, MP2 and B3LYP,

Table 4
Wiberg bond indexes (B_i), percentages of evolution through the fragmentation process (%Ev) (Eq. (6)), and synchronicities (Sy) (Eq. (3)) for TS1, TS2, TS3, TS4, TSA and TSB

		C_2N	NCl	C_1C_2	C_1O_1	C_1O_2
1	B_i^1	0.992 (1.037)	0.972 (0.924)	0.919 (0.897)	1.405 (1.452)	1.443 (1.499)
	B_i^{TS1}	1.336 (1.489)	0.504 (0.378)	0.495 (0.418)	1.587 (1.651)	1.574 (1.683)
	%Ev	36.4 (50.3)	48.1 (59.2)	46.2 (53.5)	40.2 (48.9)	30.3 (49.1)
	Sy			0.90 (0.92)		
2	B_i^2	0.972 (0.996)	0.984 (0.961)	0.907 (0.885)	1.401 (1.452)	1.458 (1.511)
	B_i^{TS2}	1.249(1.385)	0.625(0.486)	0.549(0.495)	1.552(1.629)	1.564 (1.639)
	%Ev	28.17 (40.7)	36.55 (49.4)	39.57 (44.1)	33.80 (45.0)	25.18 (33.3)
	Sy			0.91 (0.95)		
3	B_i^3	0.977 (1.039)	0.974 (0.888)	0.878 (0.802)	1.408 (1.479)	1.466 (1.527)
	B_i^{TS3}	1.208 (1.208)	0.638 (0.662)	0.589 (0.620)	1.509 (1.553)	1.547 (1.579)
	%Ev	24.6 (18.7)	34.4 (25.5)	33.0 (22.6)	23.2 (19.5)	20.5 (15.1)
	Sy			0.90 (0.92)		
4	B_i^4	0.968 (1.031)	0.972 (0.881)	0.873 (0.791)	1.407 (1.481)	1.468 (1.530)
	B_i^{TS4}	1.199(1.184)	0.635 (0.673)	0.589 (0.629)	1.509 (1.548)	1.504 (1.574)
	%Ev	23.9 (16.9)	34.7 (23.7)	32.6 (20.5)	22.6 (17.8)	18.9 (13.0)
	Sy			0.89 (0.92)		
A	B_i^A	0.970 (1.013)	0.982 (0.925)	0.903 (0.850)	1.404 (1.466)	1.462 (1.520)
	B_i^{TSA}	1.241 (1.271)	0.596 (0.586)	0.584 (0.585)	1.522 (1.578)	1.552 (1.595)
	%Ev	28.5 (28.4)	39.3 (36.6)	35.7 (31.2)	26.5 (29.3)	22.7 (22.2)
	Sy			0.91 (0.93)		
B	B_i^B	0.963 (1.016)	0.976 (0.900)	0.879 (0.807)	1.405 (1.473)	1.467 (1.530)
	B_i^{TSB}	1.204 (1.206)	0.623 (0.644)	0.585 (0.610)	1.509 (1.557)	1.549 (1.583)
	%Ev	25.2 (20.9)	36.2 (28.5)	33.5 (24.4)	23.4 (22.2)	20.8 (15.9)
	Sy			0.89 (0.92)		

Results obtained with MP2/6-31+G* computing method (in parentheses, results obtained with B3LYP/6-31+G*).

are different but with the same relationship between them. Thus, for **TS1** and **TS2**, B3LYP values are always greater than MP2 ones. The opposite trend for **TS3**, **TS4**, **TSA** and **TSB** is found.

The Grob fragmentation process for the (*N*-Cl)-2-amino alkane carboxylates present a high degree of synchronicity. Values of Sy range between 0.89–0.91 and 0.92–0.95 at MP2 and DFT methodologies, respectively. Clearly, the double bond formation $C_2{=}N$ and the N–Cl and C_1–C_2 bonds breaking take place in a slightly asynchronous manner as it was drawn from experimental data. However, it must be pointed out that the cleavage of the N–Cl bond is the more advanced molecular event at the TSs. These values range from 34.4% to 48.1% for MP2 and from 23.7% to 59.2% for B3LYP levels of calculations.

Natural population analysis shows there is a continuous flow of negative charge transfer from the carboxylate group to the chlorine fragment along the reaction pathway. At the TSs, the value of this charge process is near to 0.4 a.u.

4.2.3. Energetics and the kinetic parameters

The calculated activation parameters ($\Delta H^{\neq}$, $\Delta S^{\neq}$ and $\Delta G^{\neq}$) and the unimolecular rate coefficients (k) are listed in Table 5. Only the results obtained with the perturbation theory have been included. At MP2 level, the $\Delta H^{\neq}$ value increases from gas phase to solution up to 40 kJ mol^{-1} for **TS3**, **TS4**, **TSA** and **TSB**, 30 kJ mol^{-1} for **TS2** and only 5 kJ mol^{-1} for **TS1**. The reactants are more stabilized than the corresponding TSs, mainly due to the differences between the values of the dipole moments. MP4 activation enthalpies obtained in solution present larger values than the MP2 results. The entropic terms are calculated with MP2/6-31+G* in gas phase, thus the same value is used at all levels of calculations. The values of $\Delta S^{\neq}$ obtained for **TS1**, **TS2** and **TS3** are greater than those obtained for **TS4**, **TSA** and **TSB**.

The Gibbs free energies increase around 40 kJ mol^{-1} in **TS3**, **TS4**, **TSA** and **TSB** models in going from gas phase to solution at MP2 calculation level. In **TS1** and **TS2**, this value increases to 5 and 30 kJ mol^{-1}, respectively.

Finally, let us comment upon the values of rate coefficients. A comparison between experimental (see Table 2) and theoretical (see Table 5) results shows that only the MP4 values are in the narrow range of the experimental data for **3**, **4** and **A** systems. The theoretical values are: 0.43×10^{-2} s^{-1}, 6.1×10^{-1} s^{-1} and 1.0×10^{-3} s^{-1}, while the experimental values are: 1.12×10^{-2} s^{-1}, 1.0×10^{-1} s^{-1} and 1.5×10^{-2} s^{-1}, for **3**, **4** and **A**, respectively. A large discrepancy for the **1** system with a theoretical value of 3.49×10^{-21} s^{-1} and an

Table 5
Theoretical unimolecular rate coefficients (k), at 298.15 K, activation enthalpies ($\Delta H^{\neq}$), entropies ($\Delta S^{\neq}$) and Gibbs free energies ($\Delta G^{\neq}$) for the Grob fragmentation of (*N*-Cl)-2-amino carboxylates. Results obtained with MP2/6-31+G*gas phase (in parenthesis) and MP2/6-31+G* and MP4/6-31+G*//MP2/6-31+G* levels with the solvent effect

	$\Delta H^{\neq}$ (kJ mol^{-1})		$\Delta S^{\neq}$ (J mol^{-1} K^{-1})	$\Delta G^{\neq}$ (kJ mol^{-1})		k (s^{-1})	
	MP2	MP4	MP2	MP2	MP4	MP2	MP4
TS1	150.14 (144.89)	193.85	14.74	145.74 (140.50)	189.46	1.82×10^{-13} (1.51×10^{-12})	3.49×10^{-21}
TS2	134.11 (103.54)	147.38	13.15	130.19 (99.62)	143.46	9.65×10^{-11} (2.18×10^{-5})	4.57×10^{-13}
TS3	69.68 (30.06)	79.66	15.23	65.14 (25.52)	75.13	24.06 (2.1×10^{7})	0.43×10^{-2}
TS4	65.27 (26.66)	76.05	6.08	63.46 (24.84)	74.24	47.31 (2.7×10^{7})	6.1×10^{-1}
TSA	80.84 (41.94)	92.07	8.02	78.46 (39.55)	89.68	1.1×10^{-1} (7.31×10^{5})	1.0×10^{-3}
TSB	74.39 (33.53)	84.46	8.73	71.78 (30.93)	81.86	1.64 (2.36×10^{8})	2.8×10^{-2}

The experimental observed rate coefficients at 298 K are shown in Table 2.

experimental value of 7.2×10^{-2} s^{-1} is found. This could be explained if a cyclopropane ring breakage takes place before the Grob fragmentation. In this connection, it is worth noting that the first-order rate coefficients of **A** and **B** systems (possible products of cyclopropane breaking process) are near the experimental data obtained for **1**.

5. Conclusions

The present experimental and theoretical investigation of the decomposition process of some 2-[(*N*-Cl)-amino], $X = Cl, Br$, cyclo and acyclic alkanecarboxylates provides new insights regarding fragmentation pathways of structurally similar systems. This combined study has enabled us to establish the key factors which give rise to the molecular mechanism in these decomposition processes.

In spite of the fact that the molecular mechanism suggested by the present calculations is in agreement with the experimental observations, we do not claim that the correct activation parameters and rate coefficient can be obtained from such computing method and model used to represent solvent effects. The absolute values of these kinetic parameters may change if higher level of theory is used, and/or discrete water molecules interacting with the systems to simulate the effect of the solvent are included, and/or geometrical optimization in presence of the solvent is carried out. But, despite of these limitations, we do believe that some important features have been revealed. The results can be summarized as follows:

(i) The Grob fragmentation of (*N*-X)-2-amino cycloalkanecarboxylates takes place through an unimolecular concerted and nearly synchronous mechanism, with a TS in which the N–Cl bond breaking process is more advanced than the C_1–C_2 bond cleavage. The process yields Cl^-, CO_2 and an imine, that hydrolyzes further, leading to NH_3 and the corresponding ketone.

(ii) The kinetic parameters and the characterization of the stationary points (reactants and transition structure) have been theoretically analyzed in gas phase (B3LYP/6-31+G* and MP2/6-31+G*). To evaluate the effect of solvent in aqueous solution, self-consistent reaction field theory, as implemented in the PCM continuum method, has been used. In this case, full MP2/6-31+G* and single point energy MP4/6-31+G*//MP2/6-31+G* calculations were carried out. The first-order rate coefficient was then evaluated in terms of transition state theory and the theoretical results have been confronted with experimental data. Only the values of the rate coefficient obtained at MP4/6-31+G*//MP2/6-31+G* levels including solvent effects are within the order of magnitude of the experimental values of the rate coefficients.

(iii) Dihedral angle $\tau(ClNC_2C_1)$ associated with the antiperiplanarity between the Cl and C_1 centers is the key geometrical factor along the fragmentation process. A near antiperiplanar conformation is found in **3**, **4**, **A** and **B** compounds; while the strain of the three- and four-membered rings (**1** and **2** compounds) prevents the achievement of antiperiplanarity at the corresponding TSs.

Acknowledgements

This work was supported by the Brasilian funding agency FAPESP: Proj. 99/03097-6. J.R.S. thanks to the Generalitat Valenciana "Oficina de Ciencia y Tecnologia del Gobierno Valenciano" for visiting professor, year 2001: DOGV 3959. Computer capabilities were provided by the "Laboratório de Simulação Molecular" (Unesp, Bauru, Brazil) and "Centre d'Informàtica" (UJI, Castelló, Spain). Experimental studies were supported by the "Xunta de Galicia" (Spain), Proj. PGIDT99PX110302B.

References

[1] C.A. Grob, W. Baumann, Helv. Chim. Acta 38 (1955) 594.
[2] J. Mathieu, A. Allais, J. Valls, Angew. Chem. 72 (1960) 71.
[3] X.L. Armesto, M. Canle L., M. Losada, J.A. Santaballa, Int. J. Chem. Kinet. 25 (1993) 331.

[4] X.L. Armesto, M. Canle L., M. Losada, J.A. Santaballa, J. Chem. Soc., Perkin Trans. 2 (1993) 181.
[5] X.L. Armesto, M. Canle L., M. Losada, J.A. Santaballa, Int. J. Chem. Kinet. 25 (1993) 1.
[6] X.L. Armesto, M. Canle L., J.A. Santaballa, Tetrahedron 49 (1993) 275.
[7] X.L. Armesto, M. Canle L., M.V. García, M. Losada, J.A. Santaballa, Int. J. Chem. Kinet. 26 (1994) 1135.
[8] X.L. Armesto, M. Canle L., M. Losada, J.A. Santaballa, J. Org. Chem. 59 (1994) 4659.
[9] X.L. Armesto, M. Canle L., M.V. García, M. Losada, P. Rodríguez, J.A. Santaballa, Tetrahedron 50 (1994) 2265.
[10] X.L. Armesto, M. Canle L., A.M. Gamper, M. Losada, J.A. Santaballa, Tetrahedron 50 (1994) 10509.
[11] M. Canle L., Ph.D. Thesis, Universidade da Coruña, Spain, 1994.
[12] X.L. Armesto, M. Canle L., M. Losada, J.A. Santaballa, Bull. Soc. Chim. Fr. 132 (1995) 1061.
[13] X.L. Armesto, M. Canle L., J.A. Santaballa, in: Electronic Conference on Trends in Organic Chemistry (ECTOC-1), 1996.
[14] X.L. Armesto, M. Canle L., M.V. García, M. Losada, J.A. Santaballa, J. Phys. Org. Chem. 9 (1996) 552.
[15] X.L. Armesto, M. Canle L., M.V. García, J.A. Santaballa, Chem. Soc. Rev. 27 (1998) 453.
[16] A. Greenberg, J.F. Liebman, Strained Organic Molecules, Academic Press, New York, 1978.
[17] A. Sella, H. Basch, S. Hoz, Tettrahedron Lett. 37 (1996) 5573.
[18] A. Sella, H. Basch, S. Hoz, J. Am. Chem. Soc. 118 (1996) 416.
[19] P. Deslongchamps, Stereoelectronic Effects in Organic Chemistry, vol. 1, Pergamon Press, New York, 1983.
[20] J. Andrés, J.J. Queralt, V.S. Safont, L.M. Canle, J.A. Santaballa, J. Phys. Chem. 100 (1996) 3561.
[21] J. Andrés, J.J. Queralt, V.S. Safont, M. Canl, J.A. Santaballa, J. Phys. Org. Chem. 9 (1996) 371.
[22] J.J. Queralt, Ph.D. Thesis, Universitat Jaume I, Spain, 1996.
[23] V.S. Safont, V. Moliner, J. Andrés, L.R. Domingo, J. Phys. Chem. 101 (1997) 1859.
[24] J.J. Queralt, V.S. Safont, V. Moliner, J. Andrés, Chem. Phys. Lett. 283 (1998) 294.
[25] V.S. Safont, J. Andrés, L.R. Domingo, Chem. Phys. Lett. 288 (1998) 261.
[26] R. Stewart, The Proton: Applications to Organic Chemistry, Academic Press, Orlando, USA, 1985.
[27] F.H. Lohman, Anal. Chem. 30 (5) (1958) 972.
[28] E.C. Horning, M.G. Horning, J. Org. Chem. 11 (1946) 95.
[29] R. Grigg, M.F. Aly, V. Sridharan, S. Thianpatanagui, J. Chem. Soc. Chem. Commun. (1984) 182.
[30] H. Dakin, Biochem. J. 10 (1916) 319.
[31] H. Dakin, Biochem. J. 11 (1917) 79.
[32] W.E. Pereira, Y. Hoyano, R.E. Summons, V.A. Bacon, A.M. Duffield, Biochim. Biophys. Acta 313 (1973) 170.
[33] Z. Alouini, R. Seux, Water Res. 21 (1987) 335.
[34] A. Nweke, E. Frank, J. Scully, Environ. Sci. Technol. 23 (8) (1989) 989.
[35] B. Conyers, E. Walker, J. Scully, Environ. Sci. Technol. 27 (1993) 720.
[36] B. Conyers, E. Frank, J. Scully, Environ. Sci. Technol. 27 (2) (1993) 261.
[37] E.F. McCormick, B. Conyers, E. Frank, J. Scully, Environ. Sci. Technol. 27 (2) (1993) 255.
[38] M.J. Frisch et al., Gaussian 98, Gaussian, Inc., Pittsburgh, PA, 1998.
[39] A.D. Becke, J. Chem. Phys. 98 (1993) 5648.
[40] C. Lee, W. Yang, R.G. Parr, Phys. Rev. B 37 (1988) 785.
[41] C. Moller, M.S. Plesset, Phys. Rev. 46 (1934) 618.
[42] J. Tomasi, in: C.J. Cramer, D.G. Truhlar (Eds.), Structure and Reactivity in Aqueous Solution, American Chemical Society, Washington, 1994, pp. 10–23.
[43] J. Tomasi, M. Persico, Chem. Rev. 94 (1994) 2027.
[44] J. Baker, J. Comput. Chem. 7 (1986) 385.
[45] J. Baker, J. Comput. Chem. 8 (1987) 563.
[46] J.W. McIver Jr., Acc. Chem. Res. 7 (1974) 72.
[47] W.J. Hehre, L. Radom, P.V.R. Schleyer, J.A. Pople, Ab Initio Molecular Orbital Theory, Wiley, New York, 1986.
[48] D. McQuarrie, Statistical Mechanics, Harper & Row, New York, 1986.
[49] S. Glasstone, K.J. Laidler, H. Eyring, The Theory of Rate Processes, McGraw-Hill, New York, 1941.
[50] K.J. Laidler, Theories of Chemical Reaction Rates, McGraw-Hill, New York, 1969.
[51] B.C. Garrett, Theor. Chem. Acc. 103 (2000) 200.
[52] G.A. Petersson, Theor. Chem. Acc. 103 (2000) 190.
[53] M.G. Evans, M. Polanyi, Trans. Faraday Soc. 31 (1935) 875.
[54] H. Eyring, J. Chem. Phys. 3 (1935) 107.
[55] W.F.K. Wynne-Jones, J. Chem. Phys. 3 (1935) 492.
[56] M.G. Evans, M. Polanyi, Trans. Faraday Soc. 33 (1937) 448.
[57] M. Polanyi, J. Chem. Soc. (1937) 629.
[58] S.W. Benson, Foundations of Chemical Kinetics, McGraw-Hill, New York, 1960.
[59] C.H. Bamford, C.F.H. Tipper, in: C.H. Bamford, C.F.H. Tipper (Eds.), The Theory of Kinetics, Comprehensive Chemical Kinetics. Section 1: The Practice and Theory of Kinetics, vol. 2, Elsevier, Amsterdam, 1969.
[60] A.J.C. Varandas, S.J. Formosinho, J. Chem. Soc. Faraday Trans. 2 (82) (1986) 953.
[61] G. Lendvay, J. Mol. Struct. Theochem 167 (1988) 331.
[62] G. Lendvay, J. Phys. Chem. 93 (1989) 4422.
[63] K.B. Wiberg, Tetrahedron 24 (1968) 1083.
[64] A.E. Reed, R.B. Weinstock, F.J. Weinhold, J. Chem. Phys. 83 (1985) 735.
[65] A.E. Reed, L.A. Curtiss, F. Weinhold, Chem. Rev. 88 (1988) 899.
[66] A. Moyano, M.A. Pericàs, A. Valentí, J. Org. Chem. 54 (1989) 573.

[67] k_{obs} is used for the rate coefficient as obtained empirically, whereas k is named 'rate constant', as it is related to an elementary step. See K.J. Laider, Pure Appl. Chem. 68 (1996) 149.
[68] K.B. Wiberg, Angew. Chem. Int. Ed. Engl. 25 (1986) 312.
[69] T. Dudev, C. Lim, J. Am. Chem. Soc. 120 (1998) 4450.
[70] R. Adlington, J.E. Baldwin, B.J. Rawlings, J. Chem. Soc. Chem. Commun. (1983) 290.
[71] E. Leete, G.J. Morri, H.S.P. Rao, Rev. Latinoamer. Quím. 17 (1986) 24.
[72] G. Vaidyanathan, J.W. Wilson, J. Org. Chem. 54 (1989) 1815.
[73] M.C. Pirrung, Acc. Chem. Res. 32 (1999) 711.